

Nuclear Segmentation and Classification: On Color & Compression Generalization

Quoc Dang Vu* Robert Jewsbury* Simon Graham Mostafa Jahanifar
Shan E Ahmed Raza Fayyaz Minhas Abhir Bhalerao Nasir Rajpoot
{quoc-dang.vu, rob.jewsbury, n.m.rajpoot}@warwick.ac.uk

* Joint first authors, contributed equally

Abstract—Since the introduction of digital and computational pathology as a field, one of the major problems in the clinical application of algorithms has been the struggle to generalize well to examples outside the distribution of the training data. Existing work to address this in both pathology and natural images has focused almost exclusively on classification tasks. We explore and evaluate the robustness of the 7 best performing nuclear segmentation and classification models from the largest computational pathology challenge for this problem to date, the CoNIC challenge. We demonstrate that existing state-of-the-art (SoTA) models are robust towards compression artifacts but suffer substantial performance reduction when subjected to shifts in the color domain. We find that using stain normalization to address the domain shift problem can be detrimental to the model performance. On the other hand, neural style transfer is more consistent in improving test performance when presented with large color variations in the wild.

Index Terms—Computational Pathology, Robustness, Nuclei segmentation and classification.

I. INTRODUCTION

The spatial arrangement and morphology of nuclei are important signatures for identifying disease [1], [2]. In cancer, bio-markers such as tumor-infiltrating-lymphocytes [3] or Programmed death-ligand 1 (PD-L1) combined positive score for response to immunotherapy [4] have been found to be highly correlated with patient survival. In spite of their supposed effectiveness, their adoption and use in clinical settings remain limited due to the high degree of inter and intra observer variation [5] of the derived scores.

To overcome this limitation, many machine learning challenges [6], [7] have been proposed in digital pathology to further the innovation of automating the identification and classification of nuclei instances in Haematoxylin & Eosin (HE) stained samples. The most recent and perhaps the largest challenge of its kind to date, with 704 participants in 96 teams, the Colon Nuclei Identification and Counting Challenge 2022 (CoNIC) [8], was able to identify several powerful deep-learning-based methods for these tasks [9], [10], [11], [12], [13], [14], [15]. These methods achieved competitive performance even on an unseen, large scale cohort. While

the results are promising, it is as yet unclear whether these methods are sufficient to achieve generalization across millions of nuclei in the wild for subsequent downstream analyses.

This question about generalization in the wild is somewhat synonymous with investigating the robustness of models with respect to the shift of input distribution (or domain shift). So far in digital pathology, such investigations have been limited mostly to patch-level classification tasks [16], [17]. Concurrent to these developments, in natural images, attempts to see how deep neural networks (DNNs) fare against various input alterations have uncovered several important insights. To name a few, existing DNNs have a shape and texture bias [18], this limits the model to reason further about the geometries of their learning targets. Interestingly, this limitation relates to the commonly chosen 3×3 kernel [19].

With this perspective, it is important to gain better insights about the existing state-of-the-art (SoTA) *segmentation-based* methods for identification and classification of nuclear instances. Specifically, in this paper, we investigate how the performance of the top performing approaches in the CoNIC challenge are affected by perturbations to the input. We focus on two forms of domain shift: artifacts introduced by compressing whole slide images and alteration of image colors. We empirically show that:

- Upon the finalization of training, each approach has a virtual center of color distribution that is different from that of the training set;
- Common augmentations employed during training may not improve robustness against color and morphological perturbations as practitioners might expect;
- Stain normalization can be more detrimental to performance than beneficial and needs to be employed very carefully.

II. METHODOLOGY

A. Robustness Investigations

As noted by [20], there is no widely accepted definition for robustness. In this paper, we consider 2 aspects which determine how a sample domain becomes *shifted* compared to that of another sample and investigate how the performance of segmentation-based methods is affected in such cases: a) *Compression related artifacts* and b) *Color variation* between tissue, organs, diseases, scanning devices and staining protocols.

Q.D.Vu, R.Jewsbury, S.Graham, M.Jahanifar, S.E.A.Raza, F.Minhas, A.Bhalerao and N.Rajpoot are from the Tissue Image Analytics Centre, Department of Computer Science, University of Warwick, UK

N.Rajpoot is also affiliated with The Alan Turing Institute, London, UK and the Department of Pathology, University Hospitals Coventry & Warwickshire, UK

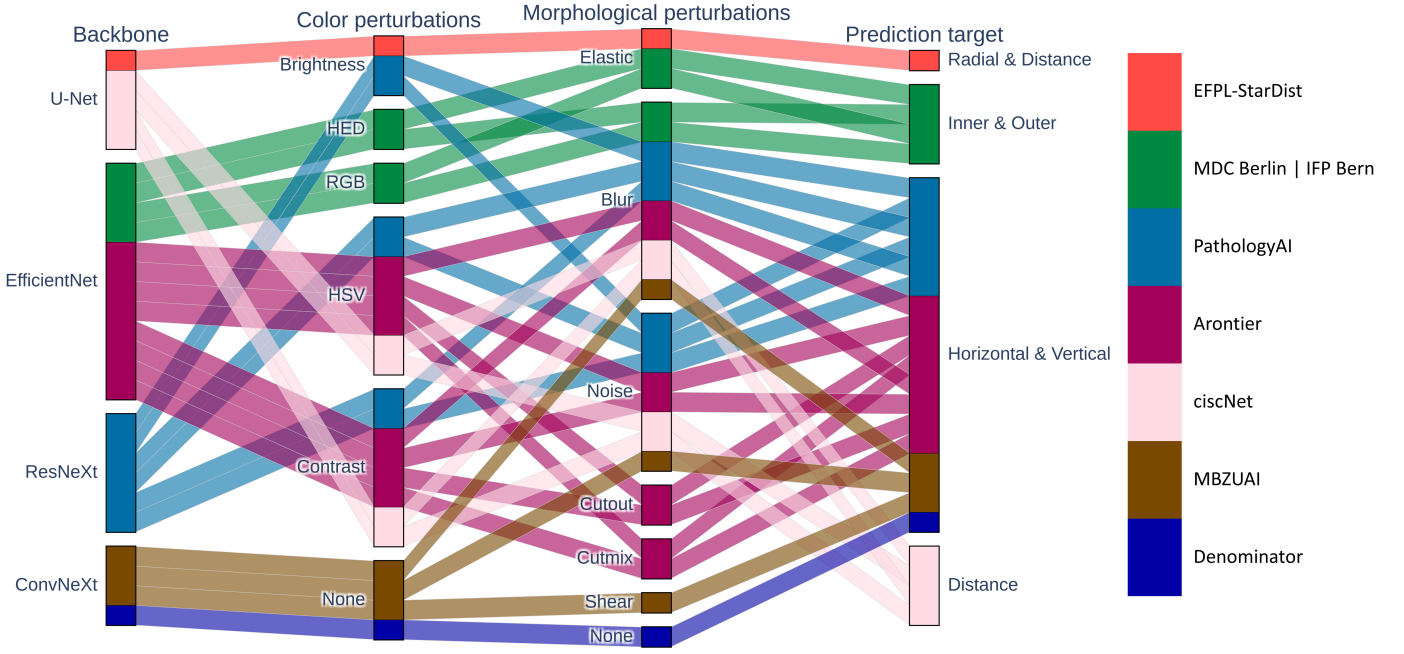


Fig. 1. Summary of assessed segmentation methods from the CoNIC challenge. Significant aspects including the backbone network family, training augmentations related to color and compression (morphology) and prediction target are shown.

B. Segmentation-based Methods

We explored the top 7 performing models in the CoNIC challenge that use a segmentation-based approach: Denominator [15], MBZUAI [12], ciscNet [14], Arontier [13], PathologyAI [9], MDC Bern - IFP Berlin [10] and EFPL - Stardist [11]. We summarize various aspects of these approaches that can influence how the models fare against the alterations under investigation in Fig. 1. All methods follow the encoder-decoder architecture paradigm and only EFPL - Stardist model was trained from scratch.

C. Evaluation Metrics

The CoNIC challenge utilized a variant of panoptic quality (PQ) [21] for multi-class problems called mPQ^+ to measure the performance of segmentation and classification of nuclei instances. At $\text{IoU}(x_t^a, y_t^a) > a$, the PQ_t^a for each type of nucleus t is defined as

$$\mathcal{PQ}_t^a = \underbrace{\frac{|TP_t^a|}{|TP_t^a| + \frac{1}{2}|FP_t^a| + \frac{1}{2}|FN_t^a|}}_{\text{Detection Quality (DQ)}} \times \underbrace{\frac{\sum_{(x_t^a, y_t^a) \in TP} \text{IoU}(x_t^a, y_t^a)}{|TP_t^a|}}{|TP_t^a|}}_{\text{Segmentation Quality (SQ)}} \quad (1)$$

Here, x_t denotes a ground truth GT (GT) instance, y_t denotes a predicted instance, and IoU denotes intersection over union. A unique pairing between a GT and predicted instance is derived when setting the threshold $a \geq 0.5$ for $\text{IoU}(x^a, y^a)$, or by using Hungarian matching for $a < 0.5$. This matching splits all available instances of type t within an image into matched pairs (TP), unmatched GT instances (FN) and unmatched predicted instances (FP). In medical images, IoU is a harsh criterion for problems that contain lots of small objects such as nuclei [22]. However, for downstream analysis, often all predicted nuclei are utilized rather than just a subset being above a certain size. We extend mPQ^+ by taking its average across a range $D = \{a \in \mathbb{R}; 0.0 \leq a \leq 0.5\}$. This is

synonymous to calculating the area under the curve (AUC), thus we define

$$mPQ^+ \text{ AUC} = \int_0^{0.5} \frac{1}{T} \sum_t^{T=6} \mathcal{PQ}_t^+ da \quad (2)$$

To reduce the computation cost, we sampled a with a step of 0.05 and used the trapezoidal rule to obtain the final results.

III. EXPERIMENTAL RESULTS

A. Dataset and Comparison Settings

Training Set: Participants in the CoNIC challenge utilized the development set of the Lizard dataset [23] for training, validating and selecting their models. In total, there are 431,913 unique nuclei belonging to 6 nuclear categories originating from 5 centers.

Testing Set: The challenge test set includes images taken from 12 different centers, where 11 of these are completely unseen in the development set. Data from these 11 centers acted as the external test set in the original Lizard publication [23]. The remaining center comprises of additional data extracted from a center that was already considered during training, but from an independent cohort. In total, there exists 103,150 unique nuclei belonging to 6 nuclear categories.

Comparison Settings: Images from both the Lizard dataset and the testing set were prepared into sets of 256×256 image patches [8]. To facilitate the discovery for new insights, the selected teams from CoNIC provided a single model that was trained, validated and selected based on a fixed split of the Lizard dataset, provided by the organizers (80/20 for training/validation). Analyses in this paper are based on these models rather than the original submissions to the challenge.

Original, Control and Assessed: We denote **Original** as the un-altered version of the test set. The whole slide images from which these patches originated could be at different

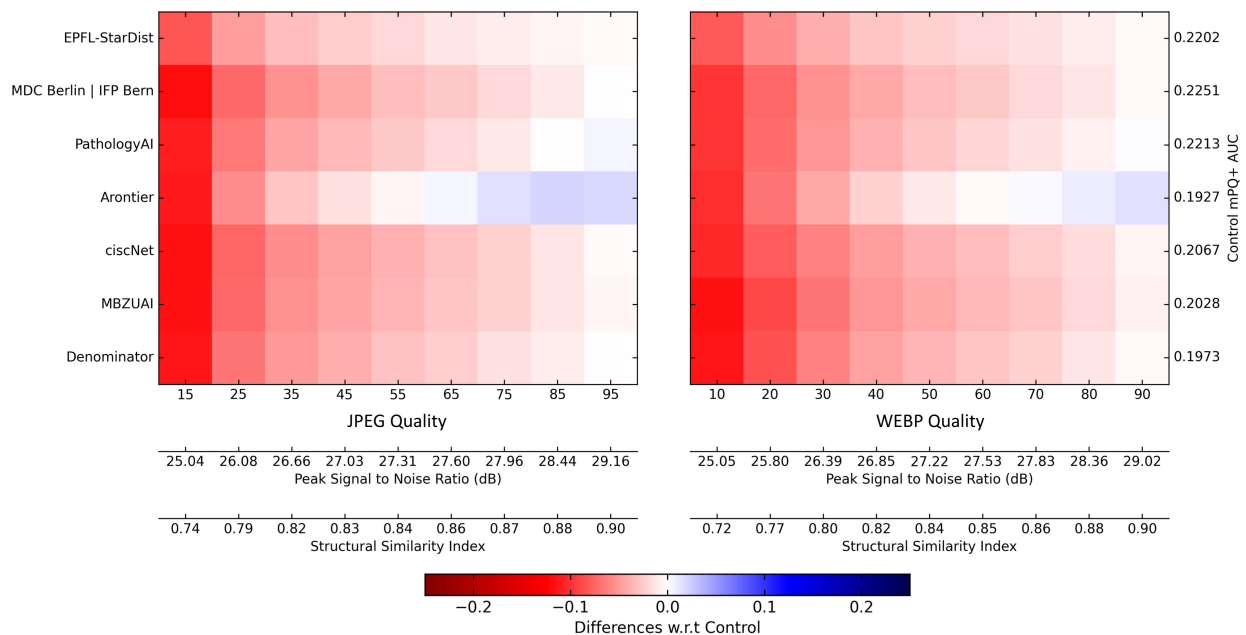


Fig. 2. Changes in the mPQ^+AUC of SoTA segmentation-based methods when varying the *quality* parameter in JPEG or WEBP compression.

resolutions and compressed by different methods, we aimed to align their information as much as possible before further compressing the data. When shifting the color domain of the test set, we found that neural style transfer[24] (neural stylization) preserves the local characteristics of the images the best at high resolution. We first created a **Control** version of the test set by up-scaling the **Original** version to super-resolution via ESRGAN [25] before resizing it back to original resolution. By perturbing this process at various stages, we obtained samples for assessing compression (compressing on **Control**) and shifting color domains (at super-resolution). We denote these versions of the test set as the **Assessed**.

B. Compression Perturbation

We evaluated two major lossy compression methods: JPEG and WEBP. We show how the performance of the selected methods varies across a range of compression qualities in Fig. 2. Intuitively, a majority of the methods experience a decrease in performance the more the images are compressed. Interestingly, the Arontier team’s model had noticeable performance gain at some compression levels compared to the **Control** results. From Fig. 1, we hypothesise this could be due to the cutout [26] and cutmix [27] augmentations they employed during training as they would introduce compression-like artifacts. None of the other teams under evaluation employed these augmentation techniques.

C. Color Perturbation

As each dataset occupies a region within a color space, visualizing how the model performances vary in such a color space is synonymous with approximating the theoretical robustness range of such a model (obtained from a specific training set) with respect to possible samples in the wild. Thus, by identifying how these changes relate to the color distribution

of the training and testing set, may provide insights on which aspect of these methods are important for generalization. To ascertain that any such observations are not restricted to a specific color space, we repeat our experiments in both the HSV and CIELAB color spaces.

Color Domains. We represent the color of each image patch by the mean of its pixel values within that color space. With these values, we establish how the entire training and test set is distributed in terms of Hue (H) and Saturation (S) for HSV or Alpha (A) and Beta (B) for CIELAB in Fig. 3 via kernel density estimation. Here, we observe that the center of the test set in CIELAB is noticeably different from that of the training set while they heavily overlap in HSV.

Color Sampling and Artificial Domain Shifting: Having defined the color domains to be investigated qualitatively in Fig. 3, further investigations required us shifting the test set toward a color value in such domain while preserving the image compositions. We achieved this by using stain-normalization or by neural stylization. Both techniques however, require a choice of reference image which represents the distribution of the domain we want to shift our target image towards.

To obtain them, we started by simplifying each color space. We restricted the value ranges of the axis within each color space such that they encapsulate the training and testing set distributions. We achieved this by setting $H \in [240, 360]$, $S \in [0.0, 1.0]$ or $A \in [0, 50]$, $B \in [-40, 10]$ based on Fig. 3. Afterward, along each axis and within these value ranges, we quantized them into 16 steps, thus creating a total of 256 sampling points (16×16) in HSV or CIELAB respectively. In other words, we obtained 256 samples within the training set which were closest to these 256 colors in each color space. Specifically, by setting the *Value* (V) and *Luminance* (L) to the mean value of the entire training set, we correspondingly obtained unique images within the training

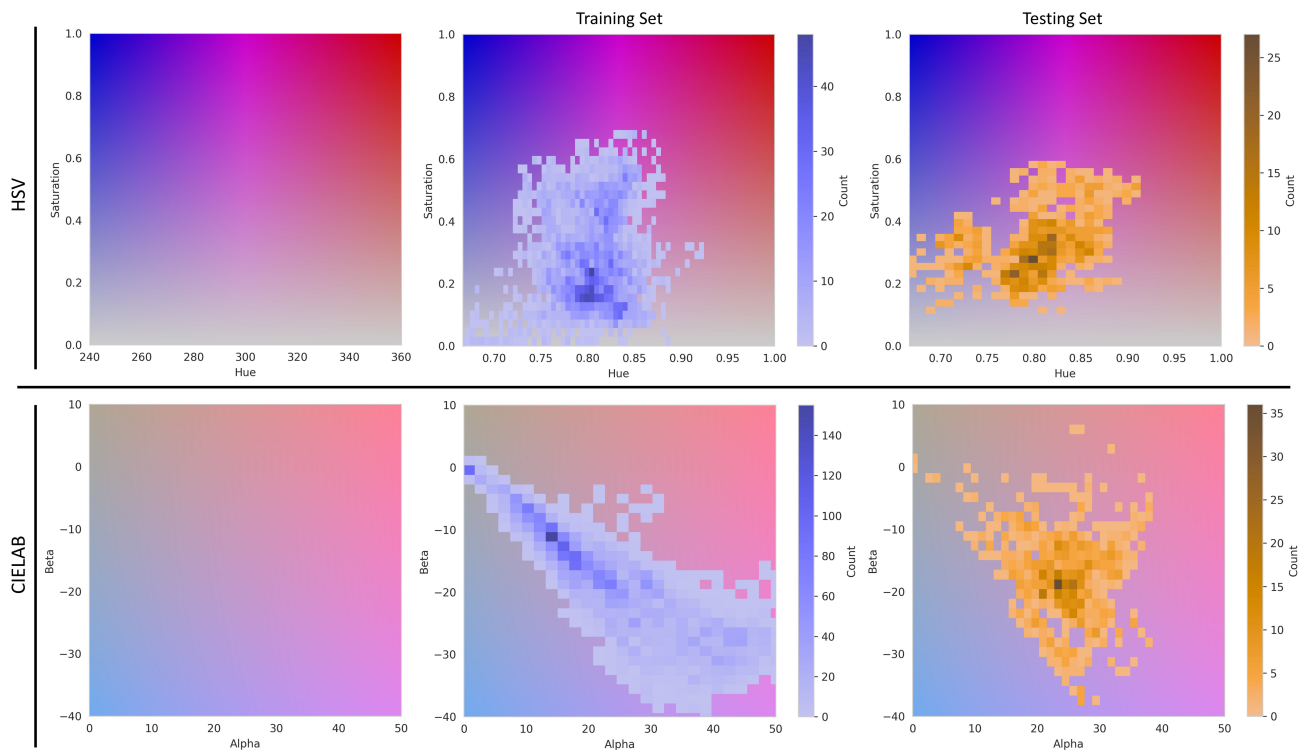


Fig. 3. Color distribution of image patches within the CoNIC training and testing set using kernel density estimation in HSV and CIELAB color space.

set that were the closest to each sampling point. Although there were 256 sampling points, the nearer towards the edge of the training distribution the sampling points became the more likely they shared the same selected images. In such cases, we only retained the ones that have smallest distance within the color space, thus obtaining 101 references for HSV and 108 for CIELAB.

Finally, because different color alteration methods behave differently, in order to ensure the validity of the observed phenomena, we also assessed the results obtained by using three different methods: Ruifrok [28] and Vahadane [29] stain-normalization and neural style transfer [24]. We provide the sampled references and a standard testing sample with their altered color in Fig. 4. Notice that each image in the figure represents a quantized color range as describe above. Additionally, for some reference images, Vahadane did not produce physically realistic samples (the teal colored images). For such cases, we excluded these from our subsequent quantitative analyses detailed in Fig. 5.

Reflected Performances: For each color alteration method, we compute the average and standard deviation of $mPQ^+ AUC$ across all versions of the testing set in each color space and plot them in Fig. 5. We observed that **Original** results are higher than that of the **Control** results. While all methods suffered to varying degrees from the color shift, MDC Bern | IFP Bern and Arontier were affected the least. Across the two color spaces and three color shift techniques, they had the overall smallest standard deviation and reduction in performance. Interestingly, we found stain-normalization to be detrimental to the model performances in general. However,

neural stylization was found to be the most stable (having the smallest deviation).

We further show how these performance changes relate to the choice of reference images for the MDC Bern | IFP Bern, Arontier and Pathology AI teams in Fig. 6. In line with our intuition, moving the color of the testing set toward the center of the training distribution can potentially improve performance, as reflected by PathologyAI. The reference images that demonstrated the smallest reduction in performance (in the case of stain-normalization) or improvement (with neural style-transfer) are found in the center of the training distribution. However, intriguingly, Arontier gained performance when the testing set moved toward areas that are not heavily populated within the training set. Meanwhile, MDC Bern | IFP Bern performed well across the range of sampled color references, with the exception of those being near the training distribution edges. We surmised this is the reason for its large deviation as seen in Fig. 5. Finally, in the context of this task, Vahadane normalization in particular is shown to be highly dependent on the choice of reference image i.e being at the center of the training distribution, regardless of the models.

IV. CONCLUSIONS

We empirically show that SoTA segmentation-based methods are quite robust against compression artifacts. If lossy compression is required, default parameters for JPEG (quality 75) and WEBP (quality 80) are sufficient. However, these models are highly volatile with respect to color variations. We find evidence that stain normalization improves model generalization. Specifically, regardless of the choice of method

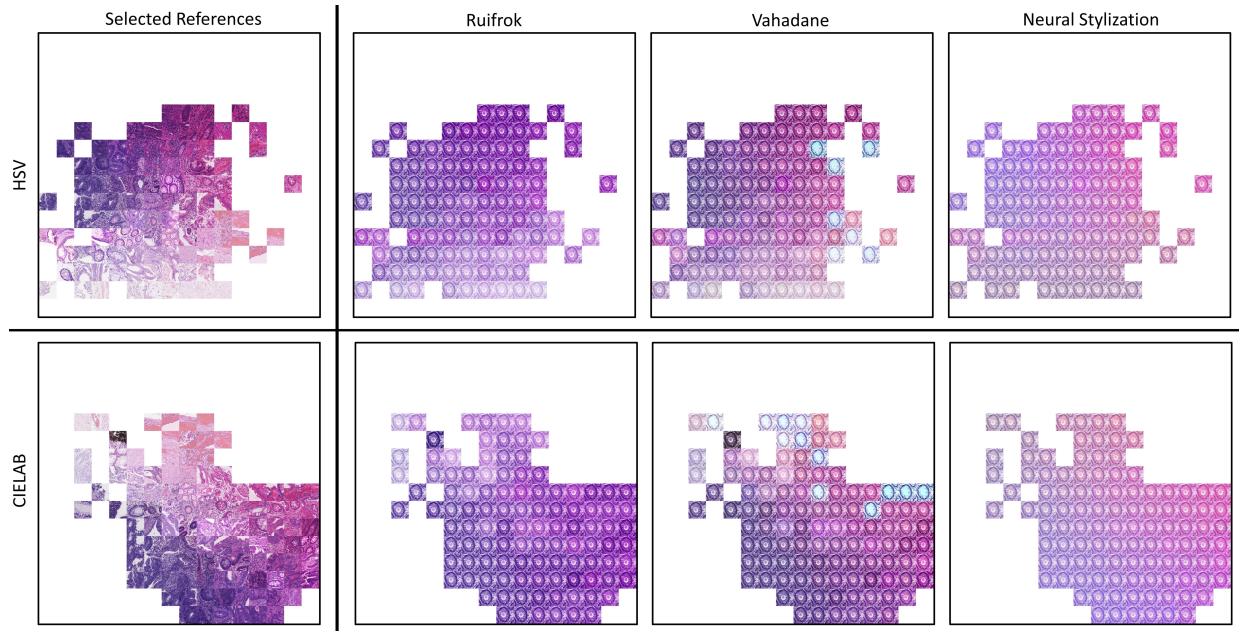


Fig. 4. Selected reference images within the training set and a test sample that has its color pulled toward the reference at the same location in HSV and CIELAB color space. The color ranges in both color space are the same as in Fig. 3.

and color space, we show that stain normalization is more likely to degrade performance than improve it. If altering the color (or stain normalization) of the dataset is required, we suggest using neural style transfer [24] as we found it to provide the most consistent gain in performance. If using stain-normalization, reference images should be from the central area of the training distribution as we found this avoids the outlier regions which resulted in substantial performance loss.

Finally, this work demonstrates that the generalization problem is a concern in spite of the improved performance of computational pathology models in nuclear classification and segmentation tasks achieved in recent years. Our findings highlight the need for further investigations into the mechanism behind these underlying problems.

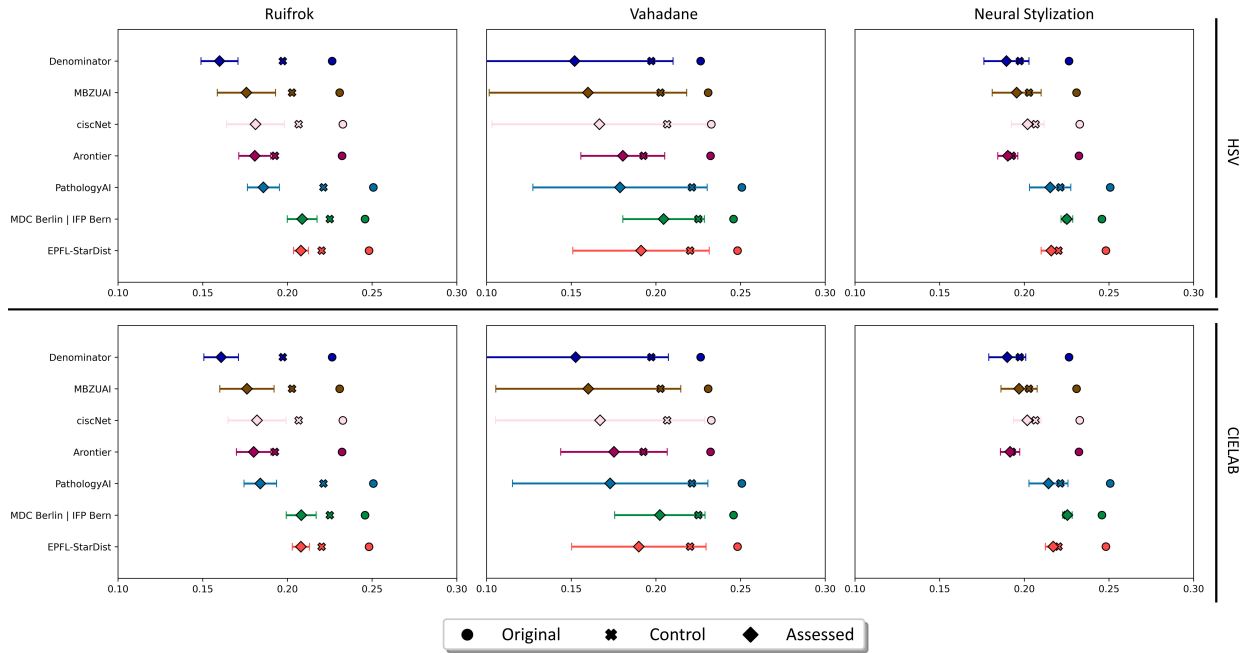


Fig. 5. Changes in the $mPQ^+ AUC$ when we artificially shifted the color of the test set using various methods. The box plots are the means and standard deviations.

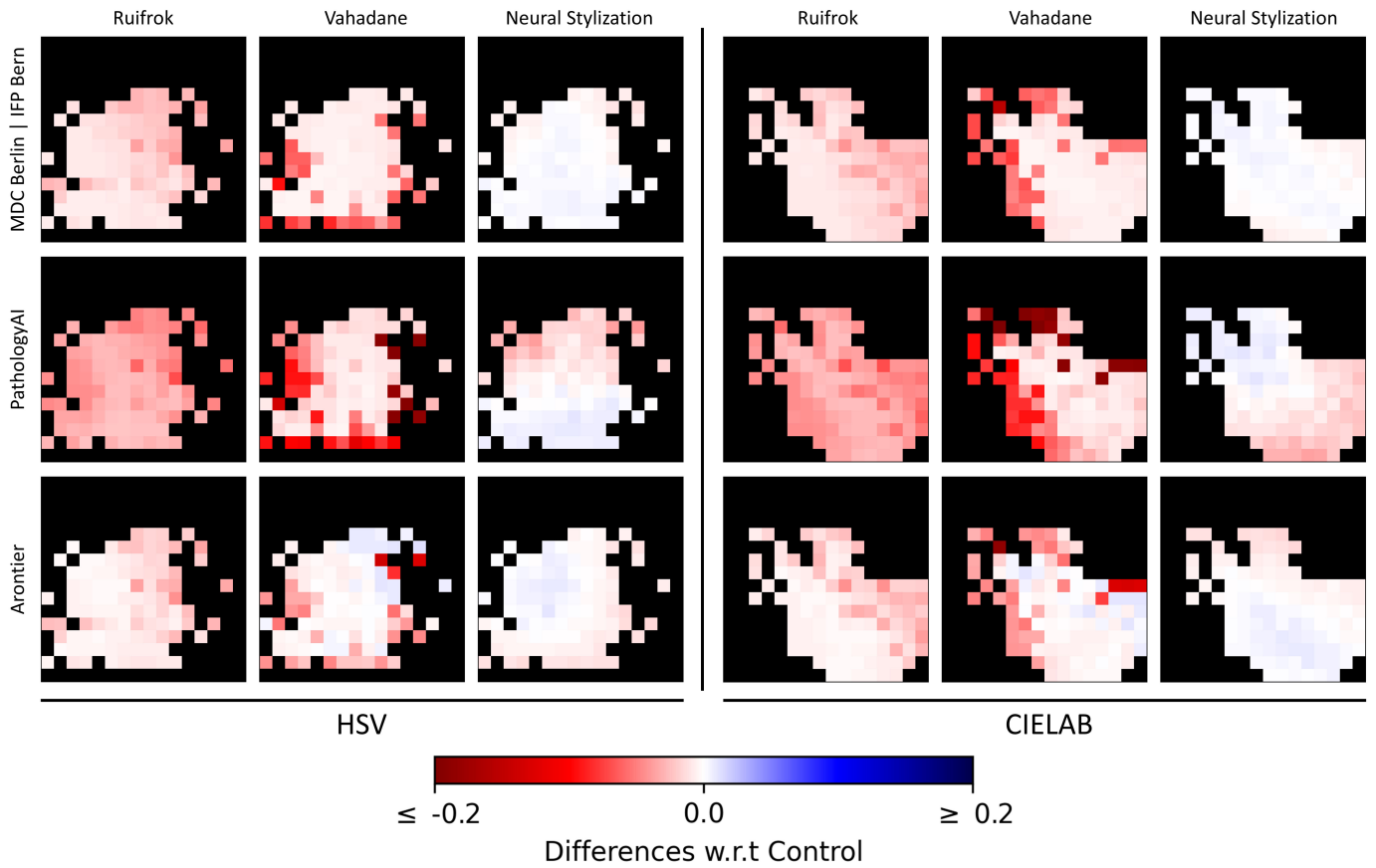


Fig. 6. Difference in the $mPQ^+ AUC$ between the **Control** and the test set where its color was shifted w.r.t. each sampled reference in Fig. 4.

REFERENCES

- [1] C. Elston and I. Ellis, "Pathological prognostic factors in breast cancer. i. the value of histological grade in breast cancer: experience from a large study with long-term follow-up," *Histopathology*, vol. 19, no. 5, pp. 403–410, 1991. [Online]. Available: <https://onlinelibrary.wiley.com/doi/abs/10.1111/j.1365-2559.1991.tb00229.x>
- [2] L. M. Solis, C. Behrens, M. G. Raso, H. Y. Lin, H. Kadara, P. Yuan, H. Galindo, X. Tang, J. J. Lee, N. Kalhor *et al.*, "Histologic patterns and molecular characteristics of lung adenocarcinoma associated with clinical outcome," *Cancer*, vol. 118, no. 11, pp. 2889–2899, 2012.
- [3] K. D. Shield, J. Ferlay, A. Jemal, R. Sankaranarayanan, A. K. Chaturvedi, F. Bray, and I. Soerjomataram, "The global incidence of lip, oral cavity, and pharyngeal cancers by subsite in 2012," *CA: a cancer journal for clinicians*, vol. 67, no. 1, pp. 51–64, 2017.
- [4] A. Fusi, L. Festino, G. Botti, G. V. Masucci, I. Melerio, P. C. Lorigan, and P. A. Ascierto, "Pd-11 expression as a potential predictive biomarker," *The Lancet. Oncology*, vol. 16, no. 13, pp. 1285–7, 2015.
- [5] T. Yamaguchi, H. Mukai, F. Akiyama, K. Arihiro, S. Masuda, M. Kurosumi, Y. Kodama, R. Horii, and H. Tsuda, "Inter-observer agreement among pathologists in grading the pathological response to neoadjuvant chemotherapy in breast cancer," *Breast Cancer*, vol. 25, no. 1, pp. 118–125, 2018.
- [6] N. Kumar, R. Verma, D. Anand, Y. Zhou, O. F. Onder, E. Tsougenis, H. Chen, P.-A. Heng, J. Li, Z. Hu *et al.*, "A multi-organ nucleus segmentation challenge," *IEEE transactions on medical imaging*, vol. 39, no. 5, pp. 1380–1391, 2019.
- [7] R. Verma *et al.*, "Monusac2020: A multi-organ nuclei segmentation and classification challenge," *IEEE Transactions on Medical Imaging*, vol. 40, no. 12, pp. 3413–3423, 2021.
- [8] S. Graham, M. Jahanifar, Q. D. Vu, G. Hadjigeorgiou, T. Leech, D. R. J. Snead, S. e Ahmed Raza, F. A. Minhas, and N. M. Rajpoot, "Conic: Colon nuclei identification and counting challenge 2022," *CoRR*, vol. abs/2111.14485, 2021. [Online]. Available: <https://arxiv.org/abs/2111.14485>
- [9] W. Zhang, "Conic solution," *arXiv preprint arXiv:2203.03415*, 2022.
- [10] J. L. Rumberger, E. Baumann, P. Hirsch, and D. Kainmueller, "Panoptic segmentation with highly imbalanced semantic labels," *arXiv preprint arXiv:2203.11692*, 2022.
- [11] M. Weigert and U. Schmidt, "Nuclei segmentation and classification in histopathology images with stardist for the conic challenge 2022," *arXiv preprint arXiv:2203.02284*, 2022.
- [12] H. Azzuni, M. Ridzuan, M. Xu, and M. Yaqub, "Color space-based hover-net for nuclei instance segmentation and classification," *arXiv preprint arXiv:2203.01940*, 2022.
- [13] H. Ahn and Y. Hong, "Class-controlled copy-paste based cell segmentation for conic challenge," *bioRxiv*, 2022.
- [14] M. Böhlend, O. Neumann, M. P. Schilling, M. Reischl, R. Mikut, K. Löffler, and T. Scherr, "ciscnet—a single-branch cell instance segmentation and classification network," *arXiv preprint arXiv:2202.13960*, 2022.
- [15] J. Li, C. Wang, B. Huang, and Z. Zhou, "Convnext-backbone hovernet for nuclei segmentation and classification," *arXiv preprint arXiv:2202.13560*, 2022.
- [16] K. Stacke, G. Eilertsen, J. Unger, and C. Lundström, "Measuring domain shift for deep learning in histopathology," *IEEE journal of biomedical and health informatics*, vol. 25, no. 2, pp. 325–336, 2020.
- [17] R. Yamashita, J. Long, S. Banda, J. Shen, and D. L. Rubin, "Learning domain-agnostic visual representation for computational pathology using medically-irrelevant style transfer augmentation," *IEEE Transactions on Medical Imaging*, vol. 40, no. 12, pp. 3945–3954, 2021.
- [18] R. Geirhos, P. Rubisch, C. Michaelis, M. Bethge, F. A. Wichmann, and W. Brendel, "Imagenet-trained cnns are biased towards texture; increasing shape bias improves accuracy and robustness," *CoRR*, vol. abs/1811.12231, 2018. [Online]. Available: <http://arxiv.org/abs/1811.12231>
- [19] X. Ding, X. Zhang, Y. Zhou, J. Han, G. Ding, and J. Sun, "Scaling up your kernels to 31x31: Revisiting large kernel design in cnns," *arXiv preprint arXiv:2203.06717*, 2022.
- [20] D. Hendrycks, S. Basart, N. Mu, S. Kadavath, F. Wang, E. Dorundo, R. Desai, T. Zhu, S. Parajuli, M. Guo, D. Song, J. Steinhardt, and J. Gilmer, "The many faces of robustness: A critical analysis of out-of-distribution generalization," *CoRR*, vol. abs/2006.16241, 2020. [Online]. Available: <https://arxiv.org/abs/2006.16241>
- [21] A. Kirillov, K. He, R. B. Girshick, C. Rother, and P. Dollár, "Panoptic segmentation," *CoRR*, vol. abs/1801.00868, 2018. [Online]. Available: <http://arxiv.org/abs/1801.00868>
- [22] Maier-Hein *et al.*, "Metrics reloaded: Pitfalls and recommendations for image analysis validation," 2022. [Online]. Available: <https://arxiv.org/abs/2206.01653>
- [23] S. Graham, M. Jahanifar, A. Azam, M. Nimir, Y.-W. Tsang, K. Dodd, E. Hero, H. Sahota, A. Tank, K. Benes *et al.*, "Lizard: A large-scale dataset for colonic nuclear instance segmentation and classification," *arXiv preprint arXiv:2108.11195*, 2021.
- [24] L. A. Gatys, A. S. Ecker, and M. Bethge, "A neural algorithm of artistic style," *CoRR*, vol. abs/1508.06576, 2015. [Online]. Available: <http://arxiv.org/abs/1508.06576>
- [25] X. Wang, K. Yu, S. Wu, J. Gu, Y. Liu, C. Dong, C. C. Loy, Y. Qiao, and X. Tang, "ESRGAN: enhanced super-resolution generative adversarial networks," *CoRR*, vol. abs/1809.00219, 2018. [Online]. Available: <http://arxiv.org/abs/1809.00219>
- [26] M. Tan and Q. Le, "Efficientnet: Rethinking model scaling for convolutional neural networks," in *International conference on machine learning*. PMLR, 2019, pp. 6105–6114.
- [27] O. Russakovsky, J. Deng, H. Su, J. Krause, S. Satheesh, S. Ma, Z. Huang, A. Karpathy, A. Khosla, M. Bernstein *et al.*, "Imagenet large scale visual recognition challenge," *International journal of computer vision*, vol. 115, no. 3, pp. 211–252, 2015.
- [28] A. C. Ruifrok, D. A. Johnston *et al.*, "Quantification of histochemical staining by color deconvolution," *Analytical and quantitative cytology and histology*, vol. 23, no. 4, pp. 291–299, 2001.
- [29] A. Vahadane, T. Peng, A. Sethi, S. Albarqouni, L. Wang, M. Baust, K. Steiger, A. M. Schlitter, I. Esposito, and N. Navab, "Structure-preserving color normalization and sparse stain separation for histological images," *IEEE transactions on medical imaging*, vol. 35, no. 8, pp. 1962–1971, 2016.